

Non-spatial symmetries in quantum nonlinear spectroscopy

Li Sun,^{1,2,3} Chong Chen,^{1,2,3} and Ren-Bao Liu^{1,2,3,4,*}

¹*Department of Physics, The Chinese University of Hong Kong,
Shatin, New Territories, Hong Kong, China*

²*The State Key Laboratory of Quantum Information Technologies and Materials,
The Chinese University of Hong Kong,
Shatin, New Territories, Hong Kong, China*

³*New Cornerstone Science Laboratory,
The Chinese University of Hong Kong,*

Shatin, New Territories, Hong Kong, China

⁴*Centre for Quantum Coherence, The Chinese University of Hong Kong,
Shatin, New Territories, Hong Kong, China*

(Dated: August 29, 2025)

Abstract

Nonlinear spectroscopy is a powerful approach to extracting information, in particular higher-order correlations of physical quantities. Quantum nonlinear spectroscopy (QNS) can access exponentially more types of correlations than its classical counterpart, since the responses to “classical forces” correspond to contour-time-ordered correlations (CTOCs) that involve only commutators, while in QNS “quantum forces” from a quantum sensor induce responses corresponding to CTOCs that involve both commutators and anti-commutators. Symmetries are important for constraining and analyzing nonlinear spectroscopy. Quantum and classical nonlinear spectroscopy have similar spatial symmetry properties. QNS, however, is expected to have its characteristic non-spatial symmetry properties since commutators and anti-commutators of physical quantities can behave differently under non-spatial transformations (such as exchange of operators). Here, we investigate how higher-order correlations extracted by QNS are constrained by non-spatial symmetries, including particle-hole (C), time-reversal (T), and their combination, i.e., chiral (S) symmetry. We find that the generalized C-symmetry imposes special selection rules on QNS, and the generalized T- and S-symmetry relate CTOCs to out-of-time-order correlations (OTOCs). This work discloses deep structures in higher-order quantum correlations due to non-spatial symmetries and provides access to certain types of OTOCs that are not directly observable.

Correlations of physical quantities are important for the study of many-body systems [1], open quantum systems [2], quantum sensing [3–6], information scrambling [7–10], and quantum foundation [11, 12]. The correlations of n physical operators $\hat{B}_1 \equiv \hat{B}_{k_1}(t_1)$, $\hat{B}_2 \equiv \hat{B}_{k_2}(t_2), \dots, \hat{B}_n \equiv \hat{B}_{k_n}(t_n)$ can be expanded in the Wightman basis [13]

$$W_n^\sigma \equiv \text{Tr} \left[\hat{B}_{\sigma(n)} \hat{B}_{\sigma(n-1)} \cdots \hat{B}_{\sigma(1)} \hat{\rho}_B \right], \quad (1)$$

where $t_1 \leq t_2 \cdots \leq t_n$, σ denotes a permutation of $(1, 2, \dots, n)$, $\hat{B}_{k_i}(t_i)$ is an operator \hat{B}_{k_i} in the interaction picture, and $\hat{\rho}_B$ denotes the initial state of the system. The dynamics of a system is fully characterized by the so-called contour-time-ordered correlations (CTOCs), in which the operators are contour-time-ordered [see Fig. 1 (a)]. As can be seen from Fig. 1 (a), the trace in Eq. (1) is the same whether the last operator B_n appears on the forward or backward branch, so there are 2^{n-1} types of n -th order CTOCs. By linear combination,

* rbliu@cuhk.edu.hk

the CTOCs can be rewritten in a more physical form as

$$C_n^\eta = \text{Tr} [\mathbb{B}_n^+ \mathbb{B}_{n-1}^{\eta_{n-1}} \cdots \mathbb{B}_2^{\eta_2} \mathbb{B}_1^{\eta_1} \hat{\rho}_B], \quad (2)$$

where the superscripts $\eta_i = \pm$ and the superoperators are defined as $\mathbb{B}^+ \hat{A} \equiv \frac{1}{2}\{\hat{B}, \hat{A}\}$ (essentially an anti-commutator) and $\mathbb{B}^- \hat{A} \equiv -i[\hat{B}, \hat{A}]$ (essentially a commutator). The term $\mathbb{B}^- \hat{\rho}_B$ represents the evolution of the target driven by the force from the quantum sensor, and $\mathbb{B}^+ \hat{\rho}_B$ has the physical meaning of the noise from the target acting on the sensor as indicated by the fact that $\text{Tr} [\mathbb{B}^+ \hat{\rho}_B] = \langle B \rangle$. The full description of the system dynamics requires CTOCs that involve both commutators and anti-commutators. For example, in the second order, the CTOC $C^{+-} = -i \langle [\hat{B}_2, \hat{B}_1] \rangle$ describes the propagation dynamics, and $C^{++} = \langle \frac{1}{2} \{ \hat{B}_2, \hat{B}_1 \} \rangle$ the fluctuation correlation. Note that these two CTOCs, through linear combination, can be transformed to the advanced and retarded Green's functions or the Keldysh-Kadanoff-Baym Green's functions [14]. In addition to CTOCs, there are $N! - 2^{N-1}$ types of N -th order correlations in which the operators appear in more than one contours of time, called rank- k out-of-time-ordered correlations (OTOCs) if k time-contours are needed [see Fig. 1(b) for an example of rank-3 OTOC] [13]. OTOCs are useful for characterizing information scrambling in quantum many-body systems [15–17].

Nonlinear spectroscopy is a widely used approach to extracting correlations. However, it can access only one type of CTOCs in each order, namely, $\text{Tr} [\mathbb{B}_{n+1}^+ \mathbb{B}_n^- \cdots \mathbb{B}_2^- \mathbb{B}_1^- \hat{\rho}_B] = (-i)^n \langle [[[\hat{B}_{n+1}, \hat{B}_n], \dots, \hat{B}_2], \hat{B}_1] \rangle$ (which involves only time-ordered commutators between the system operators) in the n -th order nonlinear response. This limitation is due to the fact that under the driving of a “classical force” $f(t)$ coupled to a “displacement” operator $\hat{B}(t)$, the evolution (and hence response) of a quantum system is governed by the commutator $-i [f(t) \hat{B}(t), \hat{\rho}_B] = -i f(t) [\hat{B}(t), \hat{\rho}_B]$. Noise spectroscopy [18–21] is another method to measure the CTOCs, but it can access only those involving solely anti-commutators (corresponding to correlations of classical noises). Though in systems at thermal equilibrium, the dissipation-fluctuation theorem can relate the two types of CTOCs in the second order [22], and it can be generalized to relate a small subset of higher-order correlations [23], the conventional nonlinear spectroscopy and the noise spectroscopy are insufficient to extract the full set of CTOCs in general. It is recently demonstrated that the quantum sensing approach can be used to extract the full set of CTOCs, which is called quantum nonlinear spectroscopy (QNS) [2, 24–26]. Yet OTOCs are not directly measurable since they are not involved in the

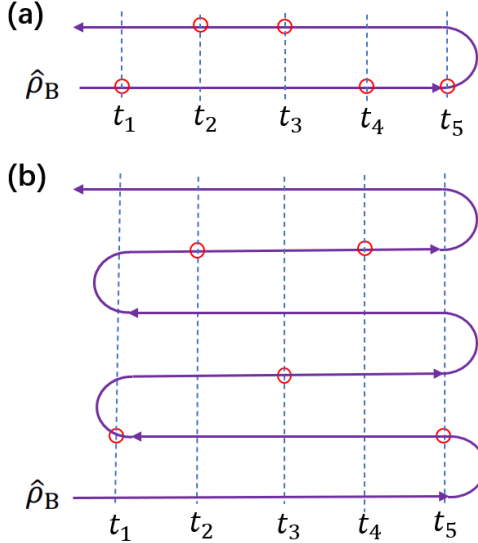


FIG. 1. Examples of the 5-th order correlations. (a) CTOC $\text{Tr}[\hat{B}_2 \hat{B}_3 \hat{B}_5 \hat{B}_4 \hat{B}_1 \hat{\rho}_B]$. In CTOCs, the operators at different times and the initial state are ordered on a contour of time, with a time-ordered sequence of operators right after the initial state on the forward branch and an anti-time ordered sequence on the backward branch. By cyclic permutation in the trace, the anti-time-ordered sequence can be placed on the right hand side of the initial state ρ_B , that is, $\text{Tr}[\hat{B}_5 \hat{B}_4 \hat{B}_1 \hat{\rho}_B \hat{B}_2 \hat{B}_3]$. (b) Rank-3 OTOC $\text{Tr}[\hat{B}_4 \hat{B}_2 \hat{B}_3 \hat{B}_1 \hat{B}_5 \hat{\rho}_B]$.

dynamics of the system. The (approximate) extraction of OTOCs requires (approximately) time-reversed evolution, which imposes a substantial experimental challenge for studying many-body systems [27–30].

Symmetry is a cornerstone of physics. The consideration of symmetry not only simplifies the analysis of systems but also constrains physical theories [31]. The symmetry analysis is particularly useful in nonlinear spectroscopy [32–35], since the higher-order responses of a system to external perturbations are complex due to the existence of many possible spatial configurations of the external forces and the responses [32]. Especially for solid-state systems, the point groups, which describe the crystallographic symmetries, simplify nonlinear spectroscopy by selection rules [32, 33].

QNS, like its classical counterpart, have structures arising from symmetries. Spatial symmetries have similar effects on quantum and classical nonlinear spectroscopy. But QNS is expected to have distinct structures due to non-spatial symmetries. For example, under matrix transpose or complex conjugation transforms, the correlations $\left\langle \frac{1}{2} \left(\hat{A} \hat{B} + \hat{B} \hat{A} \right) \right\rangle$ and

$\langle i(\hat{A}\hat{B} - \hat{B}\hat{A}) \rangle$ behave differently. Therefore, the non-spatial symmetries, such as time reversal (T), particle-hole (C), and their combination, chiral symmetry (S), are expected to induce unique structures in QNS. These non-spatial symmetries rigorously categorize Hamiltonians within the tenfold internal symmetry classes [36]. They are useful in classifying Anderson transitions [37] and topological insulators and superconductors [36], and in characterizing quantum chaos [38]. However, there is still a lack of systematic analysis of their effects on high-order quantum correlations, which is particularly relevant to QNS.

Here we study the constraints in higher-order quantum correlations imposed by non-spatial symmetries. We obtain selection rules of QNS due to C-symmetry (Theorem 1), which can reduce the number of CTOCs (among all 2^{n-1} types of n -th order CTOCs) that need to be measured. By Theorem 2 and 3, we demonstrate that T- and S-symmetry induce connections between OTOCs of different ranks (including the rank-1 OTOCs, i.e., CTOCs), which may enable the measurement of certain types of rank-2 OTOCs of T- and S-symmetric systems using QNS without the requirement of (unphysical) time-arrow reversal. We validate the structures in QNS arising from the non-spatial symmetries using the transverse-field Ising model as a case study.

A system is regarded to have *generalized* C-, T-, and S-symmetry, if the *generalized* particle-hole exchange operation (\mathcal{C}), time reversal (\mathcal{T}), or their combination ($\mathcal{S} \equiv \mathcal{C}\mathcal{T}$) correspondingly transfers its Hamiltonian H and initial state ρ_B , both being Hermitian matrices in a given basis, such that [36, 39–42]

$$\mathcal{C}H^T\mathcal{C}^{-1} = -H, \quad \mathcal{C}\rho_B^T\mathcal{C}^{-1} = \rho_B; \quad (3a)$$

$$\mathcal{T}H^*\mathcal{T}^{-1} = +H, \quad \mathcal{T}\rho_B^*\mathcal{T}^{-1} = \rho_B; \quad (3b)$$

$$\mathcal{S}H\mathcal{S}^{-1} = -H, \quad \mathcal{S}\rho_B\mathcal{S}^{-1} = \rho_B. \quad (3c)$$

Here the symmetries are called “generalized” in the sense that the transforms \mathcal{C} , \mathcal{T} and \mathcal{S} are only required to be invertible and do not need to be unitary matrices or to satisfy the conditions $\mathcal{C}\mathcal{C}^* = \pm I$, $\mathcal{T}\mathcal{T}^* = \pm I$, and $\mathcal{S}^2 = I$ [36, 39–42]. In particular, the generalized T-symmetry here does not lead to Kramers’ degeneracy.

The generalized C-symmetry leads to selection rules for high-order quantum correlations as summarized in the following theorem.

Theorem 1. *When the target system is C-symmetric and the physical quantities of interest are C-symmetric/anti-symmetric, i.e., $\mathcal{C}B_{k_i}^T\mathcal{C}^{-1} = \alpha_i B_{k_i}$ for $\alpha_i = +/ - 1$, respectively, the*

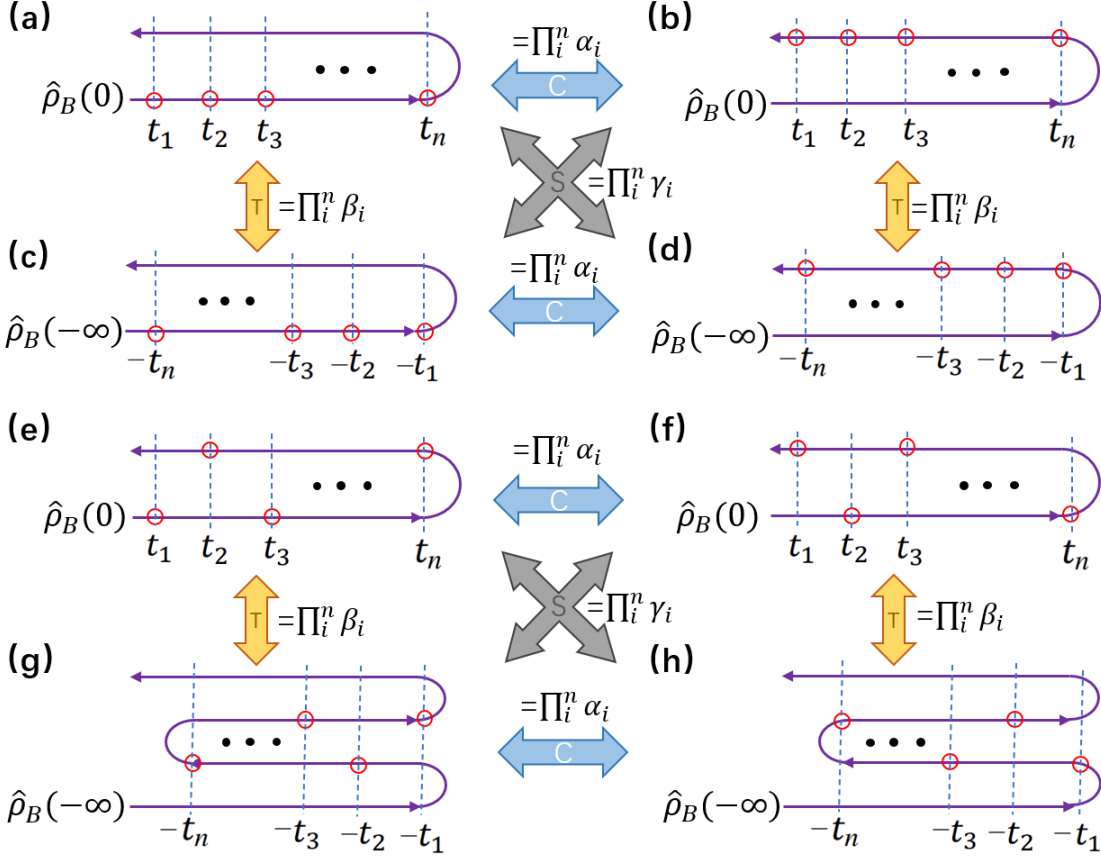


FIG. 2. Examples of rank- k Wightman correlations plotted on k time-contours and their relations induced by the C-, T- and S-symmetries. (a-d) CTOCs for operators in ascending and descending time sequences. (e-f) General rank-1 OTOCs (i.e., CTOCs). (g, h) Rank-2 OTOCs. Correlations in (a/c/e/g) are correspondingly related to those in (b/d/f/h) by \mathcal{C} -transform, (a/b/e/f) to (c/d/g/h) by \mathcal{T} -transform, and (a/b/e/f) to (d/c/h/g) by \mathcal{S} -transform, as indicated by the arrows marked by C, T, and S, correspondingly.

correlations in the Wightman basis satisfy

$$W_n^{\tilde{\sigma}} = W_n^{\sigma} \prod_{i=1}^n \alpha_i, \quad (4)$$

where $\tilde{\sigma}(i) \equiv \sigma(n - i + 1)$ denotes the reversed order of σ , and the corresponding selection rules for physical correlations are

$$C_n^{\eta} = 0 \quad \text{if} \quad \prod_{j=1}^n \eta_j + \prod_{j=1}^n \alpha_j = 0. \quad (5)$$

C-symmetry	C_2^{+-}	C_2^{++}	C_3^{+--}	C_3^{++-}	C_3^{+-+}	C_3^{+++}
$B_{k_i}^T \rightarrow -B_{k_i}$	0	-	0	-	-	0
$B_{k_i}^T \rightarrow +B_{k_i}$	0	-	-	0	0	-

TABLE I. The selection rules induced by C-symmetry in second and third-order CTOCs. 0 means the correlation must be zero.

Proof. Using the identity $\text{Tr}[A] = \text{Tr}[A^T]$, we get

$$W_n^\sigma = \text{Tr} [B_{\sigma(1)}^T B_{\sigma(2)}^T \cdots B_{\sigma(n)}^T \rho_B^T], \quad (6)$$

where $B_j^T = e^{-iH^T t_j} B_{k_j}^T e^{iH^T t_j}$. When Eq. (3a) is satisfied, it is straightforward to show that $\mathcal{C}B_j^T \mathcal{C}^{-1} = \alpha_j B_j$. Inserting $\mathcal{C}^{-1}\mathcal{C}$ between operators in Eq. (6) and using $\mathcal{C}B_j^T \mathcal{C}^{-1} = \alpha_j B_j$, we get Eq. (4). The physical correlations C_n^η are linear combinations of the Wightman correlations with the expansion coefficients associated with W_n^σ and $W_n^{\tilde{\sigma}}$ having opposite or the same sign if $||\eta||_-$, the number of $\eta_j = -$ in C_n^η , is odd or even, respectively, which leads to the selection rules in Eq. (5). \square

The relation in Eq. (4) is shown in Fig. 2 (indicated by the arrows marked by C). Note that the \mathcal{C} -transform of the correlations only switches the operators from the j -th forward/backward branch to the $(n-j+1)$ -th backward/forward one in the time-contour(s) without changing the rank of the OTOCs. The C-symmetry-induced selection rules in second- and third-order CTOCs are shown in Table I.

The generalized T-symmetry leads to the following theorem.

Theorem 2. *When the target system is T-symmetric and the physical quantities of interest are T-symmetric/anti-symmetric, i.e., $\mathcal{T}B_{k_j}^* \mathcal{T}^{-1} = \beta_j B_{k_j}$ for $\beta_j = +/ - 1$, respectively, and the system is initially in a stationary state, that is, $\rho_B(0) = \rho_B(t < 0) = \rho_B(-\infty)$, the correlations in the Wightman basis are related by*

$$W_n^\sigma = W_n^{\tilde{\sigma}}(\{t_j \rightarrow -t_j\}) \prod_{j=1}^n \beta_j. \quad (7)$$

where $\{t_j \rightarrow -t_j\}$ means that each t_j is replaced by $-t_j$ in $W_n^{\tilde{\sigma}}$.

Proof. Inserting $\mathcal{T}^{-1}\mathcal{T}$ between operators in Eq. (6) and using $\mathcal{T}e^{-iH^T t} \mathcal{T}^{-1} = \mathcal{T}e^{-iH^* t} \mathcal{T}^{-1} = e^{-iHt}$ and hence $\mathcal{T}B_{k_j}^T(t_j) \mathcal{T}^{-1} = \mathcal{T}B_{k_j}^*(t_i) \mathcal{T}^{-1} = \beta_j B_{k_j}(-t_j)$ (for B_{k_j} being Hermitian matrices), we get Eq. (7). \square

According to Eq. (7), T-symmetry transforms the operators from the j -th forward/backward branch to the $(n - j + 1)$ -th backward/forward one in the contour(s) and simultaneously changes t_i to $-t_i$, as shown in Fig. 2(c, d, g, h). After the T-transform, the time where the operators B_j occurs is $-t_j < 0$ [see Fig. 3(a)]. With the assumption that the system is initially in the stationary state such that $\rho_B(0) = \rho_B(t < 0) = \rho_B(-\infty)$, we can move the state to a time $t_0 < -t_n$ and add an empty forward (backward) branch at the beginning (end) of the time-contour to ensure that the contour always starts forward and ends backward in the initial state ρ_B [see Fig. 3(a)]. Thus, we obtain $W_n^{\tilde{\sigma}}(\{t_j \rightarrow -t_j\}) \equiv \text{Tr} [B_{\sigma(1)}(-t_{\sigma(1)}) B_{\sigma(2)}(-t_{\sigma(2)}) \cdots B_{\sigma(n)}(-t_{\sigma(n)}) \rho_B(-\infty)]$.

Interestingly, some types of CTOCs can be related to rank-2 OTOCs under the T-transform, such as the CTOCs in Fig. 2(e, f) transformed to rank-2 OTOCs in (g, h), respectively. In general, there are three different kinds of connections between OTOCs of different ranks as described below.

1. If a rank- k OTOC contains a sequence of operators in the first forward (last backward) branch of time-contour but no operators in the last backward (first forward) branch, it will be transformed by time-reversal to a rank- k OTOC with the sequence of operators in the first forward (last backward) branch reversely ordered and no operators in the last backward (first ward) branch. Examples are shown in Fig. 2(a/b) \leftrightarrow (c/d) and in Fig. 3(b).
2. If a rank- k OTOC contains operators in both the first forward and the last backward branches of time-contour, it will be transformed by time-reversal to a rank- $(k + 1)$ OTOC with no operators in either the first forward or the last backward branch. Examples are shown in Fig. 2(e/f) \rightarrow (g/h) and in Fig. 3(c).
3. If a rank- k OTOC contains no operator in either the first forward or the last backward branch of time-contour, it will be transformed by time reversal to a rank- $(k - 1)$ OTOC with operators in both the first forward and the last backward branches. Examples are shown in Fig. 2(g/h) \rightarrow (e/f) and in Fig. 3(c).

The connections among high-order quantum correlations arising from generalized S-symmetry are summarized in the following theorem.

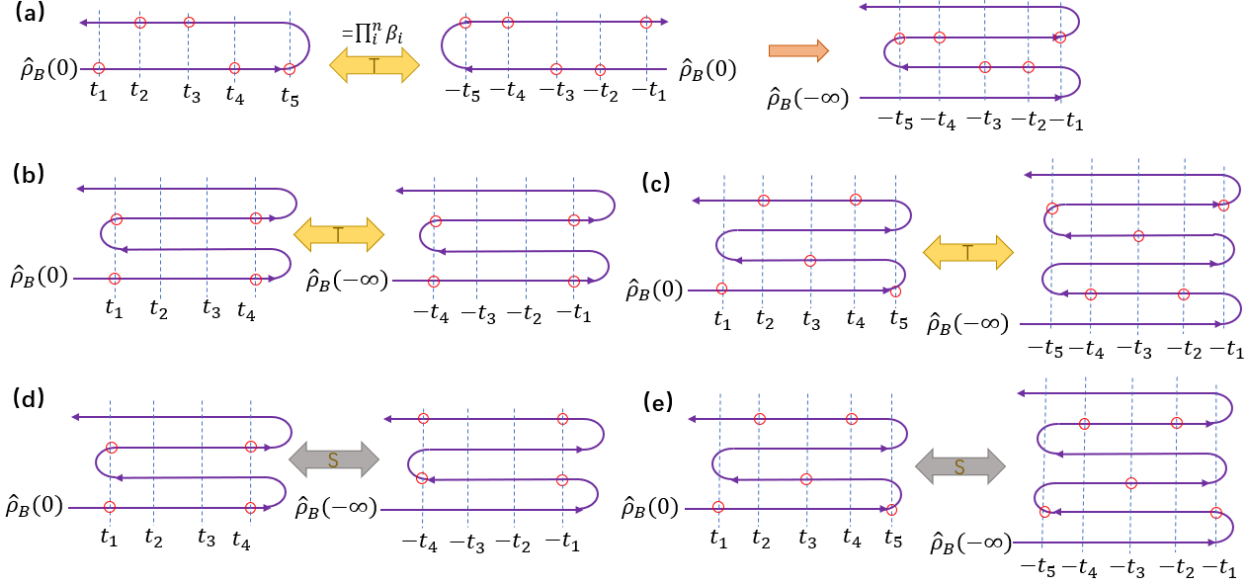


FIG. 3. OTOCs under T- and S-transforms. (a) A 5th-order CTOC is transformed to a rank-2 OTOC. When there are operators on both the first forward and the last backward branches of the time-contour, after the T-transform, two empty branches need to be added to ensure the time-contour always starts forward from and ends backward to the system state, which is assumed to be stationary so that $\rho_B(0) = \rho_B(-\infty)$. (b/d) Rank-2 OTOCs are converted into rank-2 OTOCs by T/S-transform. (c/e) Rank-2 OTOCs are converted into rank-3 OTOCs by T/S-transform.

Theorem 3. *When the target system is S-symmetric and the physical quantities of interest are S-symmetric/anti-symmetric, i.e., $\mathcal{S}B_{k_i}\mathcal{S}^{-1} = \gamma_i B_{k_i}$ for $\gamma_i = +/ - 1$, respectively, and the system is initially in a stationary state, that is, $\rho_B(0) = \rho_B(t < 0) = \rho_B(-\infty)$, the correlations in the Wightman basis are related by*

$$W_n^\sigma = W_n^\sigma(\{t_i \rightarrow -t_i\}) \prod_{i=1}^n \gamma_i, \quad (8)$$

where $\{t_i \rightarrow -t_i\}$ means that each t_i is replaced by $-t_i$ in W_n^σ .

Proof. Inserting $\mathcal{S}^{-1}\mathcal{S}$ between operators in Eq. (1) and using $\mathcal{S}B_{k_j}(t_j)\mathcal{S}^{-1} = \gamma_j B_{k_j}(-t_j)$, we get Eq. (8). \square

Similarly to the T-transform, when the system is initially in a stationary state, the S-transform also relates certain rank- k OTOCs to rank- k , rank- $(k-1)$, or rank- $(k+1)$ OTOCs, depending on whether or not there are operators in the first forward and/or the

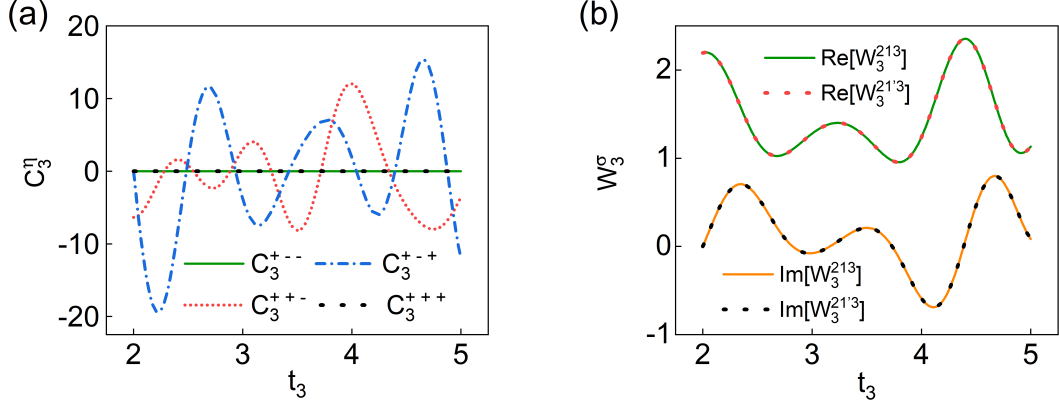


FIG. 4. Third-order correlations in transverse-field Ising model. (a) Third-order CTOCs C_3^η of C-anti-symmetric observables as functions of t_3 . (b) Real and imaginary parts of W_3^{213} and $W_3^{21'3}$ of T-symmetric observables as functions of t_3 . In the calculation, the periodic boundary condition is chosen and parameters are such that $\lambda = 1.5$, $N = 8$, $t_1 = 0$ and $t_2 = 2$.

last backward branch of the time-contour. Examples are shown in Fig. 2(a/b) \leftrightarrow (d/c) for relations between rank-1 and rank-1 OTOCs, Fig. 2(e/f) \leftrightarrow (h/g) for rank-1 \leftrightarrow rank-2 OTOCs, Fig. 3(d) for rank-2 \leftrightarrow rank-2 OTOCs, and Fig. 3(e) for rank-2 \leftrightarrow rank-3 OTOCs.

We consider the transverse-field Ising model [43] to demonstrate the above theorems. The Hamiltonian reads

$$H = - \sum_{j=1}^N \sigma_j^z - \lambda \sum_{j=1}^N \sigma_j^x \sigma_{j+1}^x,$$

where $\sigma_j^{x/y/z}$ are the Pauli matrices of the j -th spin along the $x/y/z$ axes with the basis chosen such that σ_j^z is diagonal and σ_j^x is real. With the definitions $\mathcal{C} \equiv \prod_{l=1}^{N/2} (\sigma_{2l-1}^x \sigma_{2l}^y)$ and $\mathcal{T} \equiv \prod_{l=1}^N \sigma_l^z$, the Hamiltonian has both C- and T-symmetry.

We focus on third-order correlations. To demonstrate the effects of C-symmetry, we consider a C-symmetric initial state $\rho_B = \prod_{l=1}^{N/2} [I_{2l}(\sigma_{2l-1}^x + I)/2]$ and choose a C-anti-symmetric observable $B = \frac{1}{\sqrt{N}} \sum_j \sigma_j^z$. Numerical results [Fig. 4(a)] are consistent with the selection rules for third-order CTOCs in Table I, with all terms but C_3^{+-+} and C_3^{++-} being zero. To show the effects of T-symmetry, we consider the equilibrium state $\rho_B(0) = \exp(-\beta H)/Z = \rho_B(-\infty)$ and the observable B , both being T-symmetric. As shown in Fig. 4(b), the rank-2 OTOC $W_3^{213} \equiv \text{Tr}[B(t_2)B(t_1)B(t_3)\rho_B(0)]$ and the CTOC $W_3^{21'3} \equiv \text{Tr}[B(-t_3)B(-t_1)B(-t_2)\rho_B(-\infty)] = \text{Tr}[B(t_2)B(t'_1)B(t_3)\rho_B(0)]$ (where $t'_1 \equiv t_3 + t_2 - t_1 > t_3$ and time translational invariance of the system has been used) are identical due to T-

symmetry of the system, which is consistent with Theorem 2.

In summary, we have analyzed the structures in high-order quantum correlations arising from the C-, T-, and S-symmetries. C-symmetry establishes selection rules for QNS, and T- and S-symmetries connect some types of rank-2 OTOCs to CTOCs. The connections between different ranks of OTOCs make it possible to measure certain types (but not all) of rank-2 OTOCs using QNS without the requirement of (unphysical) time-arrow reversal. They can also help reduce some higher-rank OTOCs to lower ones. Since exponential growth of OTOCs signifies information scrambling in quantum many-body systems [7–9], the connection between CTOCs and OTOCs suggests that information scrambling in quantum many-body systems is largely constrained by T- or S-symmetry, or CTOCs can exhibit diverging behaviors in T- or S-symmetric systems, which is worth further exploration.

Acknowledgments. This work was supported by the Innovation Program for Quantum Science and Technology Project No. 2023ZD0300600, the National Natural Science Foundation of China/Hong Kong Research Council Collaborative Research Scheme Project CRS-CUHK401/22, the Hong Kong Research Grants Council Senior Research Fellow Scheme Project SRFS2223-4S01, and the New Cornerstone Science Foundation.

- [1] T. Schweigler, V. Kasper, S. Erne, I. Mazets, B. Rauer, F. Cataldini, T. Langen, T. Gasenzer, J. Berges, and J. Schmiedmayer, Experimental characterization of a quantum many-body system via higher-order correlations, [Nature](#) **545**, 323 (2017).
- [2] P. Wang, C. Chen, X. Peng, J. Wrachtrup, and R.-B. Liu, Characterization of arbitrary-order correlations in quantum baths by weak measurement, [Phys. Rev. Lett.](#) **123**, 050603 (2019).
- [3] A. Laraoui, F. Dolde, C. Burk, F. Reinhard, J. Wrachtrup, and C. A. Meriles, High-resolution correlation spectroscopy of ¹³C spins near a nitrogen-vacancy centre in diamond, [Nat. commun.](#) **4**, 1651 (2013).
- [4] M. Pfender, P. Wang, H. Sumiya, S. Onoda, W. Yang, D. B. R. Dasari, P. Neumann, X.-Y. Pan, J. Isoya, R.-B. Liu, *et al.*, High-resolution spectroscopy of single nuclear spins via sequential weak measurements, [Nat. commun.](#) **10**, 594 (2019).
- [5] P. Wang, C. Chen, and R.-B. Liu, Classical-noise-free sensing based on quantum correlation measurement, [Chinese Phys. Lett.](#) **38**, 010301 (2021).

- [6] Y. Shen, P. Wang, C. T. Cheung, J. Wrachtrup, R.-B. Liu, and S. Yang, Detection of quantum signals free of classical noise via quantum correlation, *Phys. Rev. Lett.* **130**, 070802 (2023).
- [7] P. Hosur, X.-L. Qi, D. A. Roberts, and B. Yoshida, Chaos in quantum channels, *J. High Energy Phys.* **2016** (2), 4.
- [8] C. W. von Keyserlingk, T. Rakovszky, F. Pollmann, and S. L. Sondhi, Operator hydrodynamics, otocs, and entanglement growth in systems without conservation laws, *Phys. Rev. X* **8**, 021013 (2018).
- [9] G. Styliaris, N. Anand, and P. Zanardi, Information scrambling over bipartitions: Equilibration, entropy production, and typicality, *Phys. Rev. Lett.* **126**, 030601 (2021).
- [10] P. Zanardi and N. Anand, Information scrambling and chaos in open quantum systems, *Phys. Rev. A* **103**, 062214 (2021).
- [11] J. Tura, R. Augusiak, A. B. Sainz, B. Lücke, C. Klempert, M. Lewenstein, and A. Acín, Nonlocality in many-body quantum systems detected with two-body correlators, *Ann. Phys.* **362**, 370 (2015).
- [12] K. Bae and W. Son, Generalized nonlocality criteria under the correlation symmetry, *Phys. Rev. A* **98**, 022116 (2018).
- [13] F. Haehl, R. Loganayagam, P. Narayan, and M. Rangamani, Classification of out-of-time-order correlators, *SciPost Phys.* **6**, 001 (2019).
- [14] E. N. Economou, *Green's functions in quantum physics*, Vol. 7 (Springer Science & Business Media, 2006).
- [15] B. Swingle, G. Bentsen, M. Schleier-Smith, and P. Hayden, Measuring the scrambling of quantum information, *Phys. Rev. A* **94**, 040302 (2016).
- [16] H. Shen, P. Zhang, Y.-Z. You, and H. Zhai, Information scrambling in quantum neural networks, *Phys. Rev. Lett.* **124**, 200504 (2020).
- [17] J. Li, R. Fan, H. Wang, B. Ye, B. Zeng, H. Zhai, X. Peng, and J. Du, Measuring out-of-time-order correlators on a nuclear magnetic resonance quantum simulator, *Phys. Rev. X* **7**, 031011 (2017).
- [18] S. Crooker, D. Rickel, A. Balatsky, and D. Smith, Spectroscopy of spontaneous spin noise as a probe of spin dynamics and magnetic resonance, *Nature* **431**, 49 (2004).
- [19] R. Liu, S.-H. Fung, H.-K. Fung, A. Korotkov, and L. Sham, Dynamics revealed by correlations of time-distributed weak measurements of a single spin, *New J. Phys.* **12**, 013018 (2010).

[20] F. Li, S. A. Crooker, and N. A. Sinitsyn, Higher-order spin-noise spectroscopy of atomic spins in fluctuating external fields, *Phys. Rev. A* **93**, 033814 (2016).

[21] N. A. Sinitsyn and Y. V. Pershin, The theory of spin noise spectroscopy: a review, *Rep. Prog. Phys.* **79**, 106501 (2016).

[22] R. Kubo, The fluctuation-dissipation theorem, *Rep. Prog. Phys.* **29**, 255 (1966).

[23] M. Kryvohuz and S. Mukamel, Multidimensional measures of response and fluctuations in stochastic dynamical systems, *Phys. Rev. A* **86**, 043818 (2012).

[24] Z. Wu, P. Wang, T. Wang, Y. Li, R. Liu, Y. Chen, X. Peng, and R.-B. Liu, Selective detection of dynamics-complete set of correlations via quantum channels, *Phys. Rev. Lett.* **132**, 200802 (2024).

[25] J. Meinel, V. Vorobyov, P. Wang, B. Yavkin, M. Pfender, H. Sumiya, S. Onoda, J. Isoya, R.-B. Liu, and J. Wrachtrup, Quantum nonlinear spectroscopy of single nuclear spins, *Nat. Commun.* **13**, 5318 (2022).

[26] B. C. H. Cheung and R.-B. Liu, Quantum nonlinear spectroscopy via correlations of weak faraday-rotation measurements, *Adv. Quantum Technol.* , 2300286 (2023).

[27] M. Gärttner, J. G. Bohnet, A. Safavi-Naini, M. L. Wall, J. J. Bollinger, and A. M. Rey, Measuring out-of-time-order correlations and multiple quantum spectra in a trapped-ion quantum magnet, *Nat. Phys.* **13**, 781 (2017).

[28] B. Vermersch, A. Elben, L. M. Sieberer, N. Y. Yao, and P. Zoller, Probing scrambling using statistical correlations between randomized measurements, *Phys. Rev. X* **9**, 021061 (2019).

[29] A. M. Green, A. Elben, C. H. Alderete, L. K. Joshi, N. H. Nguyen, T. V. Zache, Y. Zhu, B. Sundar, and N. M. Linke, Experimental measurement of out-of-time-ordered correlators at finite temperature, *Phys. Rev. Lett.* **128**, 140601 (2022).

[30] J. Cotler, T. Schuster, and M. Mohseni, Information-theoretic hardness of out-of-time-order correlators, *Phys. Rev. A* **108**, 062608 (2023).

[31] W. Greiner and B. Müller, *Quantum mechanics: symmetries* (Springer Science & Business Media, 2012).

[32] Y.-R. Shen, *Principles of nonlinear optics* (Wiley-Interscience, New York, 1984).

[33] R. W. Boyd, A. L. Gaeta, and E. Giese, *Nonlinear optics* (Springer, 2008).

[34] R. Hellwarth, Third-order optical susceptibilities of liquids and solids, *Prog. Quantum Electron.* **5**, 1 (1977).

- [35] C. Shang and H. Hsu, The spatial symmetric forms of third-order nonlinear susceptibility, *IEEE J. Quantum Electron.* **23**, 177 (1987).
- [36] C.-K. Chiu, J. C. Y. Teo, A. P. Schnyder, and S. Ryu, Classification of topological quantum matter with symmetries, *Rev. Mod. Phys.* **88**, 035005 (2016).
- [37] F. Evers and A. D. Mirlin, Anderson transitions, *Rev. Mod. Phys.* **80**, 1355 (2008).
- [38] F. Haake, *Quantum signatures of chaos* (Springer, 1991).
- [39] A. Altland and M. R. Zirnbauer, Nonstandard symmetry classes in mesoscopic normal-superconducting hybrid structures, *Phys. Rev. B* **55**, 1142 (1997).
- [40] C. W. J. Beenakker, Random-matrix theory of quantum transport, *Rev. Mod. Phys.* **69**, 731 (1997).
- [41] C. W. J. Beenakker, Random-matrix theory of majorana fermions and topological superconductors, *Rev. Mod. Phys.* **87**, 1037 (2015).
- [42] K. Kawabata, Z. Xiao, T. Ohtsuki, and R. Shindou, Singular-value statistics of non-Hermitian random matrices and open quantum systems, *PRX Quantum* **4**, 040312 (2023).
- [43] B. K. Chakrabarti, A. Dutta, and P. Sen, *Quantum Ising phases and transitions in transverse Ising models*, Vol. 41 (Springer Science & Business Media, 2008).